Novel Quantitative Techniques in Hybrid (PET-MR) Imaging of Brain Tumors

Srinivasan Senthamizhchelvan, PhD[a],
Habib Zaidi, PhD, PD[b,c,d,*]

KEYWORDS

• PET • MRI • Hybrid imaging • Quantification • Radiation therapy • Image segmentation

KEY POINTS

- Multimodality imaging has become an integral part in the medical management of brain tumors for the past 2 decades.
- Hybrid PET-MR technology is a major breakthrough and offers many quantitative avenues for brain tumor assessment and quantification.
- In radiation oncology, image-guided patient-specific treatment planning has become a standard practice, making use of high-precision dose-delivery techniques.
- The success of image-guided radiotherapy is directly related to the accuracy of imaging methods in distinguishing tumors from surrounding normal tissues, which makes PET-MR an essential imaging modality.
- Studying tumor biology at the molecular level using PET-MR will help in charting personalized treatment plans for patients with a brain tumor and also in exploring new therapeutic opportunities in the future.

INTRODUCTION

Brain tumors are a collection of heterogeneous intracranial neoplasms, each with its own biology, treatment, and prognosis.[1] Although magnetic resonance (MR) imaging is the best imaging option for diagnosing brain tumors, understanding tumor biology at the molecular level is essential for early detection and also for delivering effective personalized treatments. Positron emission tomography (PET) is one of the most prominent molecular imaging modalities used for imaging pathophysiology of tumors at an early stage. Currently, no single imaging modality can provide the sensitivity, specificity, and high spatial resolution required in distinguishing brain tumors from surrounding normal tissues. Hence, combining anatomic and functional imaging modalities has been explored to achieve the stated goals. So far, hybrid technologies, including PET–computed tomography (CT) and PET-MR have successfully been used for brain tumor management in clinics. The quest for combined multimodality imaging is an ongoing process. In a recent study, combining MR, photoacoustics, and Raman imaging has been shown to provide promising results in identifying brain tumor margins in animal models.[2]

PET-MR has shown to be superior to CT, PET, or MR alone, mainly because it allows for molecular, anatomic, and functional imaging with uncompromised quality.[3] Tumor delineation using

[a] The Russell H. Morgan Department of Radiology and Radiological Science, Johns Hopkins University School of Medicine, Baltimore, MD, USA; [b] Division of Nuclear Medicine and Molecular Imaging, Geneva University Hospital, CH-1211 Geneva, Switzerland; [c] Geneva Neuroscience Center, Geneva University, CH-1211 Geneva, Switzerland; [d] Department of Nuclear Medicine and Molecular Imaging, University Medical Center Groningen, University of Groningen, 9700 RB Groningen, The Netherlands
* Corresponding author. Division of Nuclear Medicine, Geneva University Hospital, CH-1211 Geneva, Switzerland.
E-mail address: habib.zaidi@hcuge.ch

PET Clin 8 (2013) 219–232
http://dx.doi.org/10.1016/j.cpet.2012.09.007
1556-8598/13/$ – see front matter Published by Elsevier Inc.

the PET component with the help of high-resolution MR has proved to be advantageous compared with the use of a single modality, given the complementary information provided by each one. Imaging amino acid transport using PET tracers plays a potentially important clinical role in brain tumor detection.[4] ^{18}F-fluoro-ethyl-tyrosine (^{18}F-FET) PET demonstrated excellent results in diagnosing primary brain tumors.[5] Biologic brain tumor target volume has shown to be defined more accurately and rationally when ^{11}C-choline PET is combined with MR imaging.[6] It has been shown that ^{11}C-choline PET has a higher sensitivity and specificity in distinguishing recurrent brain tumors from radionecrosis compared with ^{18}F-fluoro-deoxy-glucose (^{18}F-FDG) PET and MR imaging.[7] The diagnostic accuracy can benefit from coregistration of PET and MR imaging, enabling the fusion of high-resolution morphologic images with corresponding biologic information. Software-based multimodality image registration for the brain has been shown to be robust and accurate and is being routinely used in the clinic for various applications, including tumor imaging.[8] These procedures are further optimized on dedicated PET-MR, systems permitting the simultaneous assessment of morphologic, functional, metabolic, and molecular information on the human brain.[9,10] In this report, we review the recent advances and clinical applications of quantitative PET-MR in brain tumor imaging.

ADVANCES IN HYBRID PET-MR INSTRUMENTATION FOR BRAIN IMAGING

From the Limited Role of CT in PET-CT to the Promise of MR in PET-MR

The introduction of combined PET-CT scanners was an instant game changer in medical imaging and has superseded standalone PET scanners. Integrated PET-CT scanners allowed the overlay of sequentially acquired CT and PET images and have been a practical and viable approach in obtaining coregistered functional and anatomic images in a single scanning session. However, for brain imaging, the poor soft tissue contrast of CT has long been a drawback. This has been one of the compelling reasons for integrating high-resolution anatomic information from MR imaging with the functional PET information. Initially, intramodality image registration methods were used and were found to be inadequate, which prompted the idea of simultaneous PET-MR prototypes for animal imaging.[11] PET has very high sensitivity for tracking biomarkers *in vivo* but has poor resolving power for morphology, whereas MR imaging has lower sensitivity, but produces high soft tissue contrast. Combining PET and MR imaging in a single platform to harness the synergy of these 2 modalities is very intuitive and logical. The synergy of PET-MR has proven very powerful in studying biology and pathology in the preclinical setting and has great potential for clinical applications.[12] A typical example in which PET-MR plays a key role over PET-CT is illustrated in **Fig. 1**. PET-MR overcomes many limitations of PET-CT, such as limited tissue contrast and high radiation doses delivered to the patient or the animal being studied.[13] In addition, recent PET-MR designs allow for simultaneous rather than sequential acquisition of PET and MR imaging data, which could not have been achieved through a combination of PET and CT scanners.[14]

Dedicated Brain PET-MR Instrumentation

Hybrid PET-MR technology was initially developed for imaging small animal models of human disease,[11,12,15,16] and through many years of technical improvements was shown to be feasible in imaging the human brain[17,18] and the whole body.[14,19] Combining PET and MR for simultaneous acquisition of spatially and temporally correlated PET-MR data sets is technically challenging owing to the strong magnetic fields in the MR subsystem. Despite the challenges and technical difficulties, a clinical PET-MR prototype (BrainPET, Siemens Medical Solutions, Erlangen, Germany) dedicated for simultaneous PET-MR brain imaging was developed and installed in a few institutions for validation and testing.[17] The system was assessed in clinical and research settings in 5 academic institutions in Germany and the Unites States by exploiting the full potential of anatomic MR imaging in terms of high soft tissue contrast sensitivity in addition to the many other possibilities offered by this modality, including blood oxygenation level–dependent imaging, functional MR imaging, diffusion-weighted imaging, perfusion-weighted imaging, and diffusion tensor imaging.[20] A second sequential combined PET-MR system was also designed for molecular-genetic brain imaging by docking separate PET and MR systems together so that they share a common bed that passes through the field of view of both cameras.[21] This was achieved by combining 2 high-end imaging devices, namely a high-resolution research tomograph and a 7-T MR image with submillimeter resolution.

Dedicated PET-MR is a valuable tool for grading of brain tumors, detection of recurrences, and monitoring treatment response. MR imaging alone is not sufficient in applications, such as defining tumor infiltration boundaries and therapy response evaluation wherein biologic changes precede

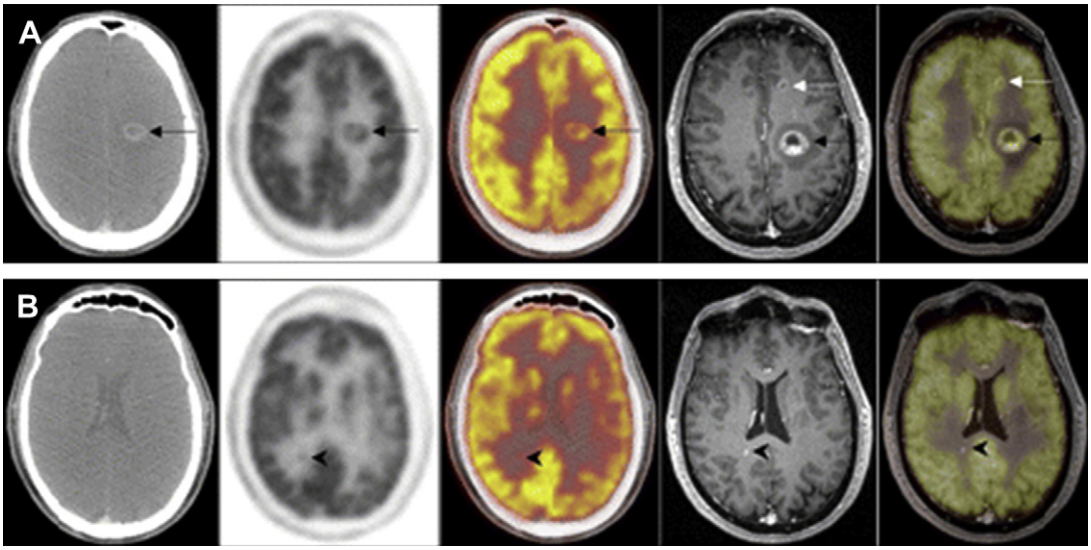

Fig. 1. A 54-year-old patient with cerebral metastases from cancer of unknown primary. (*A*) Large left-hemisphere metastasis (*black arrow*) is visible on (from left to right) axial contrast-enhanced CT, ^{18}F-FDG PET, PET-CT, axial contrast-enhanced MR imaging, and PET/MR imaging, whereas smaller metastasis of left frontal lobe (*white arrow*) is visible solely on MR imaging and PET/MR imaging. Location of this metastasis directly adjacent to highly ^{18}F-FDG–avid cortex leads to problems with diagnosing this lesion on ^{18}F-FDG PET scan. (*B*) Another subcentimeter-sized metastasis of right temporal lobe, clearly visible on MR imaging and PET/MR imaging of same patient (*arrowhead*), was only retrospectively seen as faintly increased ^{18}F-FDG activity on ^{18}F-FDG PET and PET-CT because of lack of anatomic correlate on CT. (*Adapted from* Buchbender C, Heusner TA, Lauenstein TC, et al. Oncologic PET/MRI, Part 1: tumors of the brain, head and neck, chest, abdomen, and pelvis. J Nucl Med 2012;53(6):928–38; with permission.)

morphologic signals. **Fig. 2** shows representative clinical brain PET-CT and PET-MR images of a healthy subject acquired sequentially on 2 combined systems, namely the Biograph TrueV (Siemens Healthcare, Erlangen, Germany)[22] and Ingenuity TF PET-MRI (Philips Healthcare, Eindhoven, The Netherlands).[19] The PET-CT study was started 30 minutes following injection of 370 MBq of ^{18}F-FDG followed by PET-MR imaging, which started about 80 minutes later. The better soft tissue contrast observed on MR imaging is obvious and further emphasizes the ineffectiveness of PET-CT for this indication and the potential role of PET-MR imaging.[23,24]

INNOVATIONS IN MR IMAGING–GUIDED QUANTITATIVE BRAIN PET IMAGING

PET-MR imaging has primarily been used to fuse functional/molecular and anatomic data to facilitate anatomic localization of functional abnormalities and also to aid in quantitative analysis of specific regions of interest or at the voxel level. In addition, anatomic information derived from MR imaging might also be useful for attenuation correction, motion compensation, scatter modeling and correction, and partial volume correction and could serve as *a priori* information to guide the PET reconstruction process. In spite of the widespread interest in PET-MR imaging, there are several challenges that face the use of PET-MR in clinical settings.

MR Imaging–Guided Attenuation Correction in PET-MR

Quantitative measurement of PET radiotracer activity concentration requires correction for photon attenuation and much of PET-MR success in the future will likely depend on the accuracy of determining an attenuation map from the MR signal. Because of space constraints, a transmission scan system can hardly be fit inside a PET-MR scanner, although a recent study reported on the placement of an annulus Ge-68 transmission source inside the field of view of the PET detector ring, thus enabling simultaneous acquisition of 511-keV photons emanating from the patient and the transmission source.[25] Time-of-flight information is used to discriminate the coincident photons originating from the transmission source. Unlike PET-CT, attenuation correction in PET-MR systems is not trivial because the MR signal reflects tissue proton densities and relaxation times and

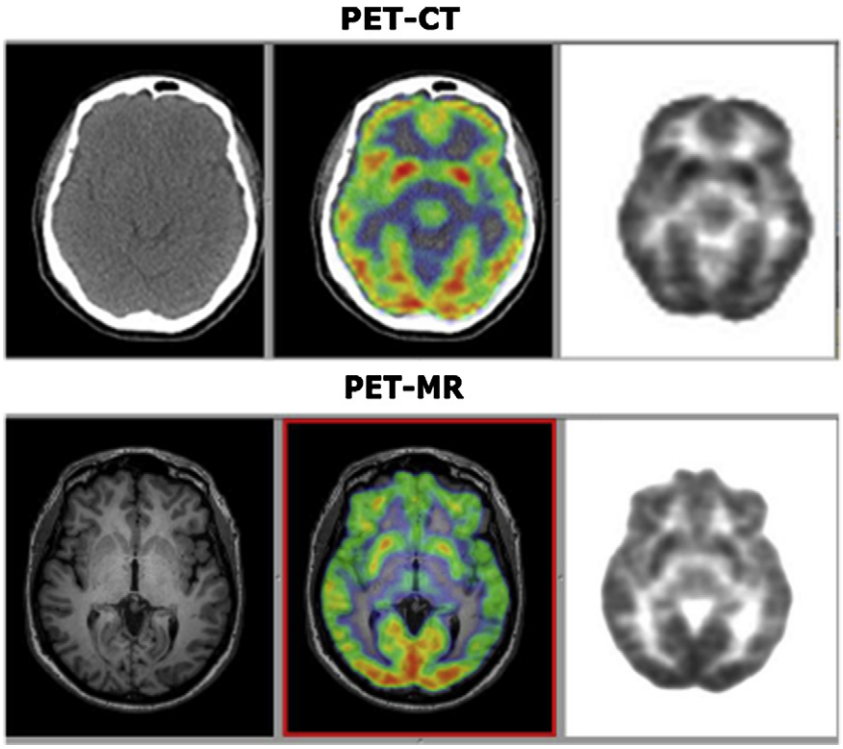

Fig. 2. Representative clinical PET-CT (*top row*) and PET-MR (*bottom row*) brain images of a healthy subject acquired sequentially (~80-minute time difference) on 2 combined systems (Siemens Biograph TrueV and Philips Ingenuity TF PET-MRI, respectively) following injection of 370 MBq of ^{18}F-FDG. (*Courtesy of* Geneva University Hospital.)

not electron density. Moreover, MR signals are not directly related to the tissue attenuation.[26] This becomes a limiting issue in locating and mapping bone, brain skull, lungs, and other unpredictable benign or malignant anatomic abnormalities with varying densities. Bone is intrinsically not detectable by conventional MR sequences, as it shows up as a black or void region, which makes it difficult to distinguish bone from air. In the head, however, the skull bone is covered by subcutaneous fat and encloses the brain. Incorporation of *a priori* anatomic knowledge allows for sufficient information to be collected to precisely segment MR scans and thus to provide an accurate attenuation map.

Various approaches have been used to derive the attenuation map from MR images.[27] Segmentation of gray matter, white matter, and water equivalent soft tissue structures are relatively trivial but it is highly challenging to segment bone tissue from air-filled spaces using conventional MR sequences. Zaidi and colleagues[28] have developed an MR-guided attenuation correction technique for brain PET imaging to alleviate the requirement of acquiring an x-ray CT scan using fuzzy logic segmentation. Using segmented T1-weighted 3-dimensional MR images, the investigators have shown the possibility of deriving a nonuniform attenuation map from MR imaging for brain PET imaging. The procedure was further refined by automating the segmentation of the skull procedure of T1-weighted MR image using a sequence of mathematical morphologic operations.[29] A proof of principle of the use of dual-echo ultra-short echo time MR imaging–based attenuation correction in brain imaging to discriminate air-filled cavities from bone on MR images was also reported.[30,31]

An alternative to the image segmentation approach is the use of anatomic atlas registration for attenuation correction where the PET atlas is registered to the patient's PET and prior knowledge of the atlas' attenuation properties is used to build a patient-specific attenuation map.[32] Deformable image registration plays a key role in atlas-based attenuation correction, which may fail in situations with large deformations. Moreover, it is not clear to what extent global anatomy from an atlas could realistically predict an individual patient's attenuation map. Hofmann and colleagues[33] studied an MR-guided attenuation correction technique using image segmentation and a method based on an atlas registration

and pattern recognition (AT&PR) algorithm in 11 patients and reported that the MR-guided technique using AT&PR provided better overall PET quantification accuracy than the basic MR image segmentation approach because of the significantly reduced volume of errors made regarding volumes of interest within or near bones and the slightly reduced volume of errors made regarding areas outside the lungs. Marshall and colleagues[34] developed a technique wherein variable lung density was taken into account in the attenuation correction of whole-body PET-MR imaging. The investigators first established a relationship between MR imaging and CT signal in the lungs and used it to predict attenuation coefficients from MR imaging. They reported that their technique improved the quantitative fidelity of PET images in the lungs and nearby tissues compared with an approach that assumes uniform lung density. Recently, Chang and colleagues[35] investigated the use of nonattenuated PET images as a means for attenuation correction of PET images in PET-MR systems using a 3-step iterative process and suggested that the technique is feasible in the clinics and can potentially be an alternative method of MR-based attenuation correction in PET-MR imaging.

Fig. 3 illustrates different ways of deriving the attenuation map for brain PET imaging including transmission scanning, model or atlas-based approaches, x-ray CT, segmented T1-weighted MR imaging, and more sophisticated MR imaging–guided derivation of the attenuation map. **Fig. 3** also shows the transaxial CT cross section, the corresponding coregistered MR imaging cross section, and the segmented MR image required in generating a 3-tissue compartment head model corresponding to brain, skull, and scalp using the algorithm mentioned previously.[36] Compensation for attenuation in the bed and head holder can be accomplished as

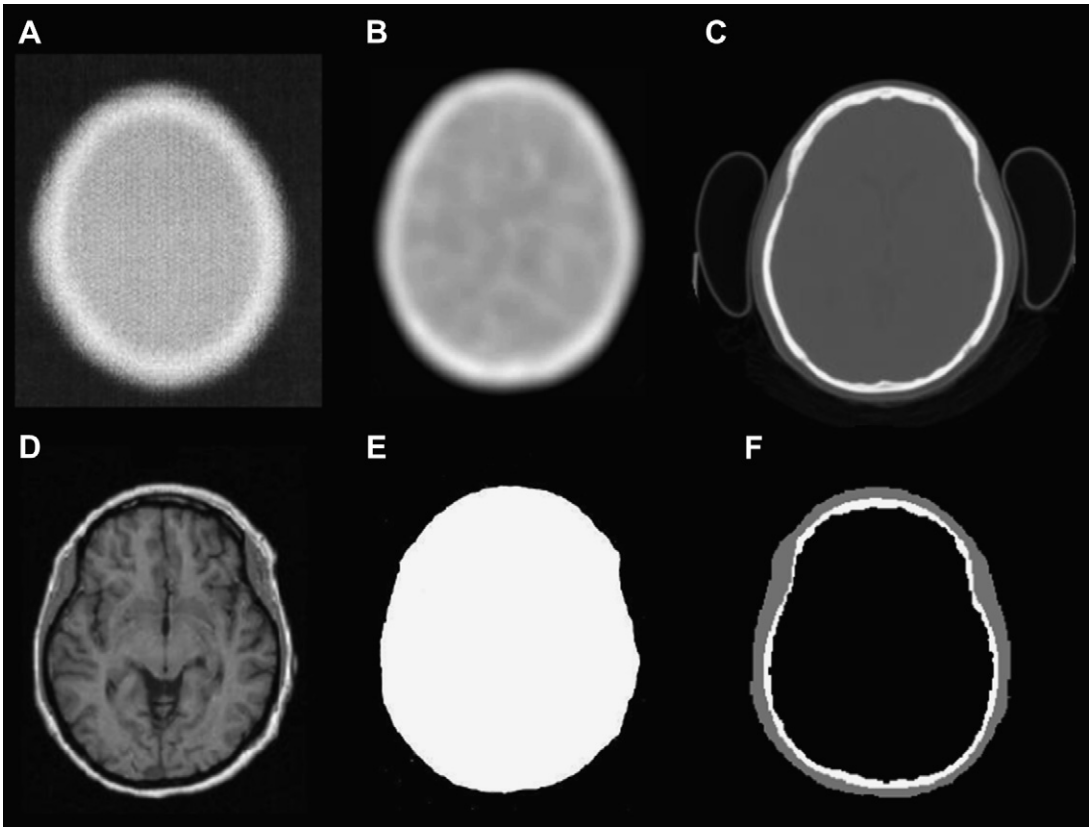

Fig. 3. Illustration of different techniques used to determine the attenuation map of the brain, including (*A*) model-based techniques producing a 3-class attenuation map, (*B*) transmission scan, (*C*) X-ray CT transaxial cross section and its corresponding coregistered MR imaging cross section (*D*), the segmented MR imaging required to generate a single-class (*E*) by thresholding and 3-class compartment head model corresponding to brain, skull and scalp. (*F*) White voxels are labeled as skull, dark gray voxels are labeled as scalp, and intracranial black voxels are labeled as brain tissue.

discussed previously for calculated attenuation correction methods.[29]

Many challenging issues, such as contrast instability of MR in comparison with CT, inaccuracies associated with assigning theoretical or uniform attenuation coefficients, motion artifacts, and attenuation of MR hardware, still need to be addressed adequately.[24] MR-guided attenuation correction is clearly evolving and will remain a hot topic that requires further research and development efforts. Apparent other advantages of MR are in motion correction and in partial volume correction of PET data.

MR Imaging–Guided PET Image Reconstruction and Partial Volume Correction

Statistical methods have been increasingly used in PET image reconstruction because of their better noise properties. In addition, information regarding the image formation and physics processes can be incorporated using Bayesian *priors*. However, an undesirable by-product of the statistical iterative reconstruction techniques, such as maximum likelihood-expectation maximization algorithm (ML-EM), is that large numbers of iterations are prone to increase the noise content of the reconstructed PET images. In emission tomography, photon noise is modeled as having a Poisson distribution. The noise characteristics can be overcome by incorporating *a priori* distribution to describe the statistical properties of the unknown image and thus produce *a posteriori* probability distributions from the image conditioned on the data. Bayesian reconstruction methods form a logical extension of the ML-EM algorithm. Maximization of the *a posteriori* (MAP) probability over the set of possible images results in the MAP estimate. This approach has many advantages, as various components of the prior, such as pseudo-Poisson nature of statistics, non-negativity of the solution, local voxel correlations, or known existence of anatomic boundaries may be added individually in the practical implementation of the algorithms.[37]

Using a Bayesian resolution loss model in PET images can be avoided by incorporating prior anatomic information from a coregistered MR or CT image in the PET reconstruction process. Combined PET-CT and PET-MR systems produce accurately registered anatomic and functional image data that can be exploited in developing Bayesian MAP reconstruction techniques.[38] PET image reconstruction using MAP has been shown to have improved contrast versus noise tradeoff.[39] In brain imaging, MR imaging–guided PET image reconstruction was reported to outperform CT-guided reconstruction owing to the high soft tissue contrast provided by MR and the accuracy obtained using sophisticated brain MR imaging segmentation procedures.[40]

The quantitative accuracy of PET activity concentration estimates for sources having dimensions less than twice the system's spatial resolution is limited because the counts in smaller volumes are spread over a larger volume than the physical size of the object owing to the limited spatial resolution of the imaging system. This phenomenon is referred to as the partial volume effect (PVE) and can be corrected using one of the various strategies developed for this purpose. In multimodality brain imaging, a main concern has been related to the PVE correction for cerebral metabolism in the atrophied brain, particularly in Alzheimer disease (AD). The accuracy of MR imaging–guided PVE correction in PET largely depends on the accuracy achieved by the PET-MR imaging coregistration procedure, which is improved by using simultaneous hybrid PET-MR imaging systems. Zaidi and colleagues[40] evaluated the impact of brain MR image segmentation methods on PET partial volume correction in ^{18}F-FDG and ^{18}F-L-dihydroxyphenylalanine (^{18}F-DOPA) brain PET imaging. The results indicated that a careful choice of the segmentation algorithm should be made while using geometric transfer matrix–based partial volume corrections in brain PET.

Fig. 4 illustrates the impact of PVE correction in functional FDG-PET brain imaging of a patient with suspected AD.[23] The voxel-based MR imaging–guided PVE correction applied here follows the approach by Matsuda and colleagues.[41]

Recently, Wang and Fei[42] introduced a PVE correction method that incorporates edge information in MR imaging to guide PET partial volume correction without MR imaging segmentation taking advantage of the PET-MR alignment. The second issue affecting the accuracy of MR imaging–guided partial volume correction in brain PET is the MR segmentation procedure. In this context, the high soft tissue contrast of MR allows the differentiation between gray and white matter. Shidahara and colleagues[43] studied a wavelet transform–based synergistic approach that combines functional and structural information from a number of sources (CT, MR imaging, and anatomic probabilistic atlases) for the accurate quantitative recovery of radioactivity concentration in PET images. The study demonstrated that the synergistic use of functional and structural data yields morphologically corrected PET images of high quality. Le Pogam and colleagues[44] proposed a voxel-wise PVE correction based on the original mutual multiresolution analysis approach (MAA). The study showed an improved and more robust

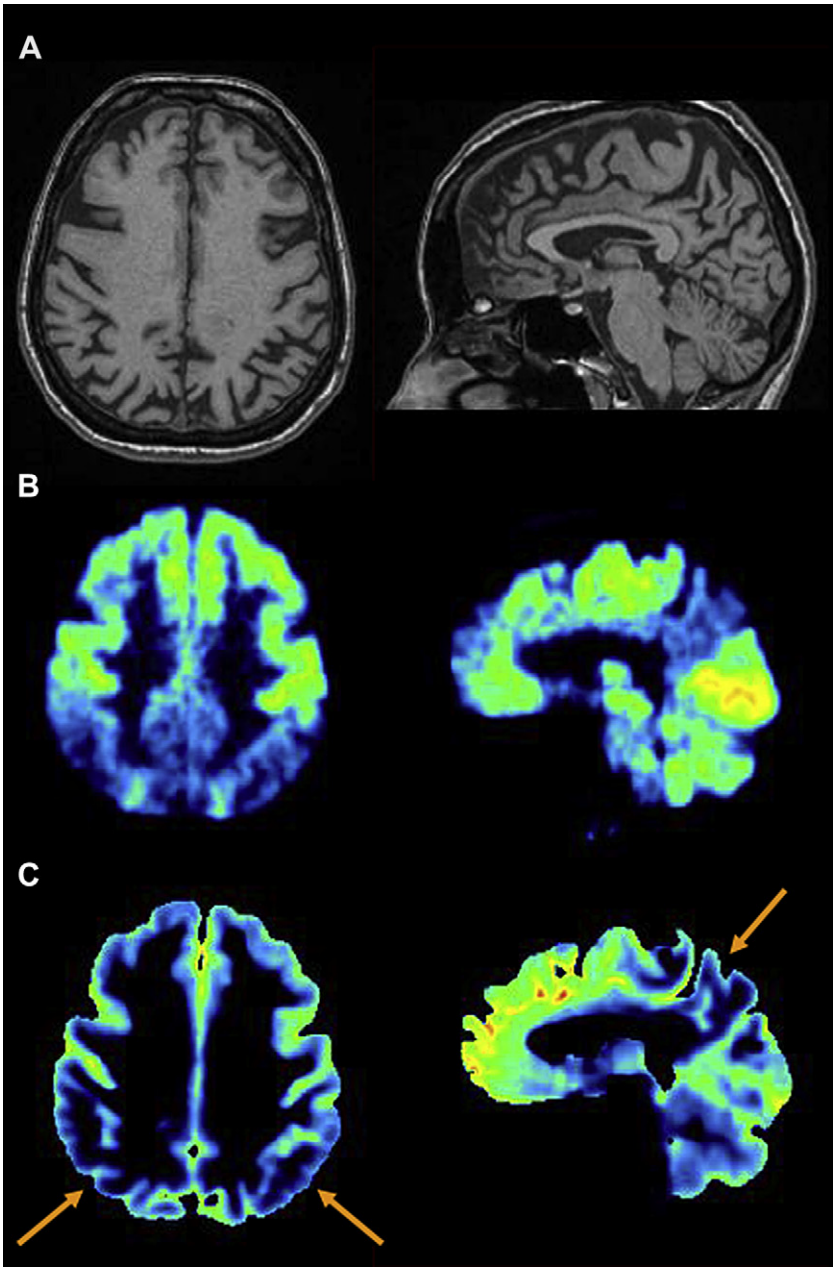

Fig. 4. Illustration of MR imaging–guided partial volume correction impact in functional brain PET imaging showing for a patient with probable Alzheimer's disease the original T1-weighted MR image (*A*) and PET image before (*B*) and after partial volume effect correction (*C*). The arrows put in evidence that the hypometabolism extends beyond the atrophy.

qualitative and quantitative accuracy compared with the MAA methodology, particularly in the absence of full correlation between anatomic and functional information.

MR Imaging–Guided Motion Correction

The intrinsic spatial resolution achieved using high-resolution PET scanners available today does not translate into spatial resolution achieved in the clinical imaging because of various factors, including motion during or between the anatomic and functional image acquisitions.[45] Patient motion (voluntary or involuntary)–related quantitative inaccuracy is common in imaging the brain, head and neck, thoracic, and abdomen regions because of long PET acquisition time. Although

the common misalignment between PET and CT images in the thoracic region on combined PET-CT scanners is related to differences between breathing patterns and acquisition times, this challenging issue will likely be addressed partly in some cases, but not necessarily in all, through the introduction of PET-MR because of the longer acquisition time of typical MR sequences used for attenuation correction, thus leading to temporal averaging and improvement in the alignment between MR imaging and PET.

In brain PET-MR prototype scanners, rigid-body[46] and nonrigid motion correction[47] methods have been successfully tested for improved spatial resolution and accurate PET quantification. Tsoumpas and colleagues[48] studied the potential of using MR-derived motion fields to correct nonrigid motion in PET and showed that combined PET-MR acquisitions could potentially allow motion compensation in whole-body PET acquisitions without prolonging acquisition time or increasing radiation dose. In neurologic simultaneous PET-MR studies, Catana and colleagues[49] showed, using 3-dimensional Hoffman brain phantom and human volunteer studies, that high temporal-resolution MR imaging–derived motion estimates acquired simultaneously on the hybrid brain PET-MR scanner can be used to improve PET image quality, therefore increasing its reliability, reproducibility, and quantitative accuracy. Imaging *in vivo* primates, Chun and colleagues[47] have recently shown that tagged MR imaging–based motion correction in simultaneous PET-MR significantly improves lesion detection compared with respiratory gating and no motion correction while reducing radiation dose.

ROLE OF HYBRID PET-MR FOR TARGET VOLUME DELINEATION OF BRAIN TUMORS

Rationale Behind the Use of PET in Biologic Tumor Volume Delineation

In radiotherapy treatment planning, the identification of gross tumor boundaries, known as gross tumor volume (GTV), is the first essential step. Knowledge of anatomic and functional tumor extent with respect to surrounding normal tissue is essential in GTV delineation. In brain tumors, the identification of aggressive tumor components within spatially heterogeneous lesions is challenging.[50] MR imaging allows precise information on tumor morphology but fails to provide details on tumor activity and metabolism. PET helps in tumor grading, assessing tumor extent, and in studying metabolism. As such, combined PET-MR reins in the synergy and helps in personalized radiotherapy treatment planning in brain tumors.[51]

In the radiotherapy treatment planning of glioblastoma multiforme (GBM), MR imaging is routinely used for GTV delineation. One of the caveats in using MR imaging for delineating glioma tumor boundaries is that MR imaging is unreliable mainly because of the inherently infiltration nature of GBM and the lack of distinction between glioma and surrounding edema with MR imaging. Increasing evidence suggests that brain tumor imaging with PET using amino acids is more reliable than MR imaging to define the extent of cerebral gliomas.[5,6,52] **Fig. 5**. is an example of the applicability and clinical usefulness of combined PET-MR in the imaging of brain tumors.

PET Image Segmentation Techniques

Identifying a perfect image segmentation algorithm in the absence of the ground truth and considering the imperfect system response function is a challenge in PET quantification. In addition, the low spatial resolution and high noise characteristics of PET images makes image segmentation a difficult task. Image segmentation is defined as the process of classifying the voxels of an image into a set of distinct classes. Image segmentation has been identified as the key problem of medical image analysis and remains a challenging and fascinating area of research. Despite the difficulties and known limitations, several image segmentation approaches have been proposed and used in the clinical setting, including thresholding, region growing, classifiers, clustering, edge detection, Markov random field models, artificial neural networks, deformable models, atlas-guided, and many other approaches.[53]

Manual segmentation methods available on most commercial software packages to identify lesion boundaries and to quantify GTVs in terms of standardized uptake value are very laborious and tedious. They discourage physicians from taking advantage of the inherently quantitative data and compel them to use qualitative means in their diagnosis, therapy planning, and assessment of patient response to therapy. Semiautomated or fully automated segmentation methods enable physicians to easily extract maximum and mean standardized uptake value estimates from a lesion volume. This also allows the physician to track changes in lesion size and uptake after radio/chemotherapy. At present, various methods are used in practice to delineate PET-based target volumes.[53]

Manual delineation of target volumes using different window-level settings and look-up tables is the most common and widely used technique in the clinic; however, the method is highly

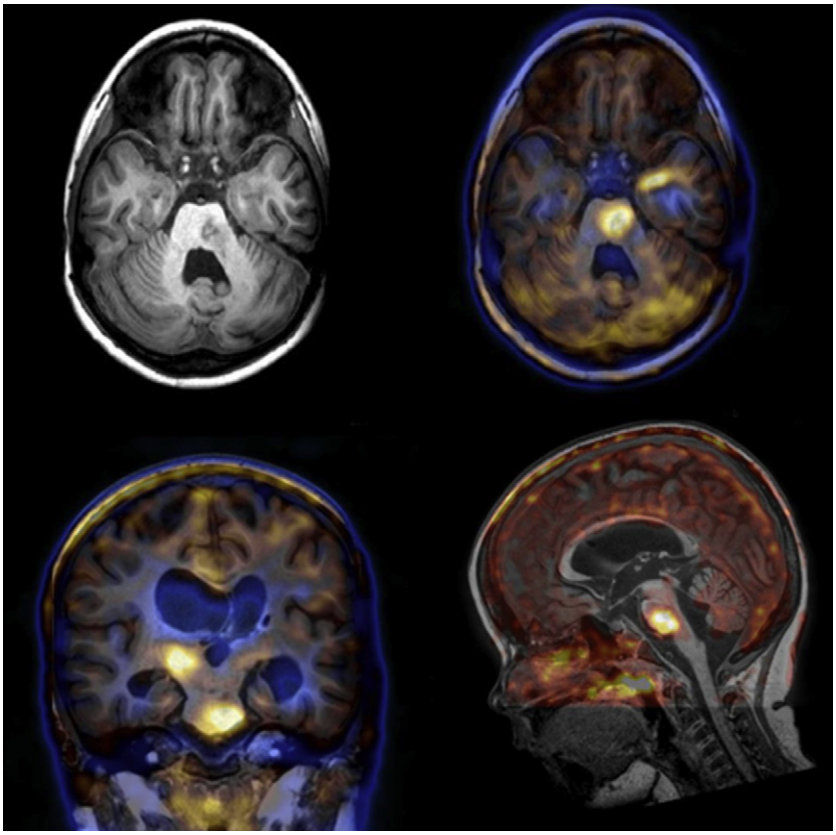

Fig. 5. Transaxial ^{18}F-FET PET-MR images of a 7-year-old girl with carcinoma of the choroid plexus (*top row*). The exact localization of the tumors is pinpointed on the fused coronal/sagittal PET-MR images (*bottom row*). (*Courtesy of* Geneva University Hospital.)

operator-dependent and is subject to high variability among operators. Rather large intraobserver variability was reported[54] for many localizations, including high-grade glioma (HGG), as shown in **Fig. 6**. In this respect, semiautomated or fully automated delineation techniques might offer several advantages over manual techniques by reducing operator error/subjectivity, thereby improving reproducibility. Our group reported on the contribution of ^{18}F-FET PET in the delineation of GTV in patients with HGG as compared with MR imaging alone using manual and semiautomated techniques.[55] In this study, PET-based tumor volumes were delineated in 18 patients using 7 image-segmentation techniques. The PET image-segmentation techniques included manual delineation of contours ($GTV_{(man)}$), a 2.5 standardized uptake value (SUV) cutoff ($GTV_{(2.5)}$), a fixed threshold of 40% and 50% of the maximum signal intensity ($GTV_{(40\%)}$ and $GTV_{(50\%)}$), signal-to-background ratio (SBR)-based adaptive thresholding ($GTV_{(SBR)}$), gradient find ($GTV_{(GF)}$), and region growing ($GTV_{(RG)}$). Overlap analysis was also conducted to assess geographic mismatch between the GTVs delineated using the different techniques. Contours defined using $GTV_{(2.5)}$ failed to provide successful delineation technically in 3 patients (18% of cases) as SUV(max) less than 2.5 and clinically in 14 patients (78% of cases). Overall, most GTVs defined on PET-based techniques were usually found to be smaller than $GTV_{(MR\ imaging)}$ (67% of cases). Yet, PET frequently detected tumors that were not visible on MR imaging and added substantial tumor extension outside the $GTV_{(MR\ imaging)}$ in 6 patients (33% of cases). The study showed that the selection of the most appropriate ^{18}F-FET PET-based segmentation algorithm is crucial, as it affects both the volume and shape of the resulting GTV. The SBR-based PET technique was shown to be useful and suggested that it may add considerably important information on tumor extent to conventional MR imaging–guided GTV delineation.

Amino Acids in Brain Gliomas

Amino acid (AA)-based PET tracers (AA-PET) L-methyl-[C-11]methionine (MET), and ^{18}F-FET

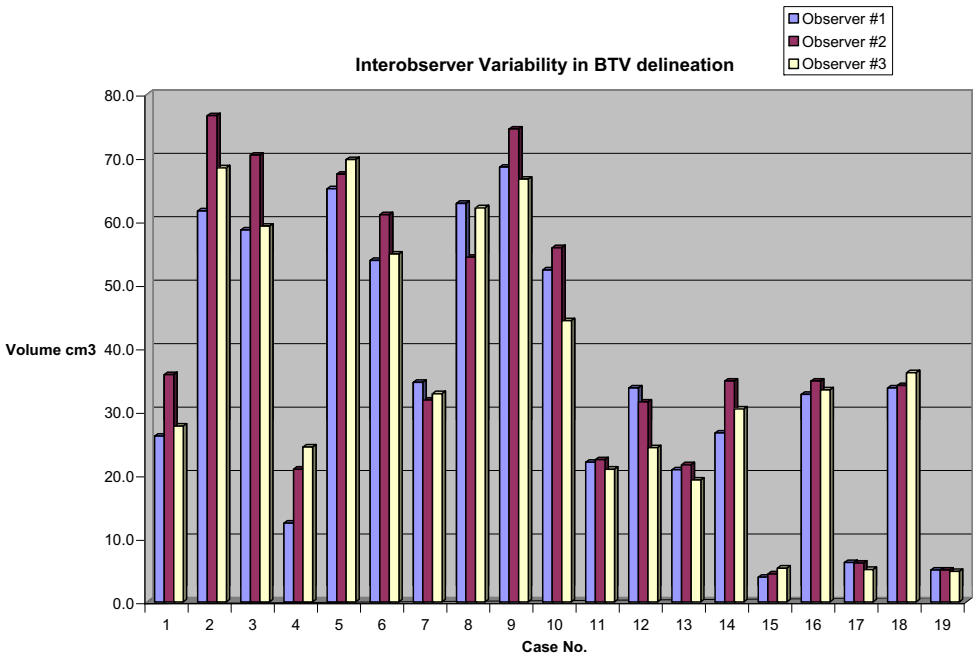

Fig. 6. Interobserver variability in biologic tumor volume delineation by 3 observers for each high-grade glioma case (1 through 19). (*Adapted from* Zaidi H, Senthamizhchelvan S. Assessment of biologic target volume using positron emission tomography in high-grade glioma patients. In: Hayat E, editor. Tumors of the central nervous system. vol. 2. New York: Springer; 2011:131–41.)

have shown higher sensitivity and specificity (85%–95%) for malignant gliomas in comparison with MR imaging. MET-PET and FET-PET have shown to have similar tumor uptake patterns.[56] AA-PET has been gaining interest and is routinely being performed to differentiate viable tumor form radiation-induced necrotic regions. In GTV delineation, AA-PET is used to determine tumor extent. Grosu and colleagues[57] showed the utility of MET-PET and iodo-methyl-tyrosine single-photon emission computed tomography (SPECT) for GTV delineation in gliomas. An increase in median survival from 6 months to 11 months has been reported in patients with recurrent high-grade gliomas whose radiotherapy treatment was planned on the basis of biologic imaging using MET-PET or SPECT in comparison with those patients whose treatment was planned conventionally.[58] Galldiks and colleagues[59] studied treatment response in patients with glioblastoma using ^{18}F-FET PET alongside MR imaging and showed that in comparison with MR imaging tumor volumes, changes in ^{18}F-FET PET may be a valuable parameter to assess treatment response in glioblastoma and to predict survival time. This study and other studies have exemplified the relevance of metabolically active tumor volumes in AA-PET to assess treatment response.[59,60] **Fig. 7** demonstrates a typical case in which PET plays an important role in delineating biologically active tumor volume over MR alone.

Other Relevant Tracers for Brain Tumor Imaging

Tumor hypoxia remains the most challenging condition for treatment. Although oxygen metabolism in gliomas differs from that of normal brain tissue, the lack of oxygen appears to be an important factor in determining glioma aggressiveness and response to therapy. It has been documented in several types of cancers that low levels of oxygen tension are associated with persistent tumor following radiation therapy and with the subsequent development of local recurrences. In gliomas, spontaneous necrosis suggests the presence of hypoxic regions that are radioresistant. Most of the PET tracers for tumor hypoxia are from the family of 2′-nitroimidazole compounds, which exhibit a rate of uptake that is purely dependent on the oxygen concentration.[61] Currently available hypoxia-imaging agents include, but not are limited to, ^{18}F-fluoroazomycinarabinofuranoside (^{18}F-FAZA), and its iodinated counterparts (^{123}I/^{124}I-IAZA), ^{18}F-fluoromisonidazole (^{18}F-MISO), ^{64}Cu-diacetyl-bis(N4-methylthiosemicarbazone) (^{64}Cu-ATSM), or ^{99m}Tc-labeled and ^{68}Ga-labeled metronidazole. The role of hypoxia imaging in measuring the extent of tumor hypoxia,

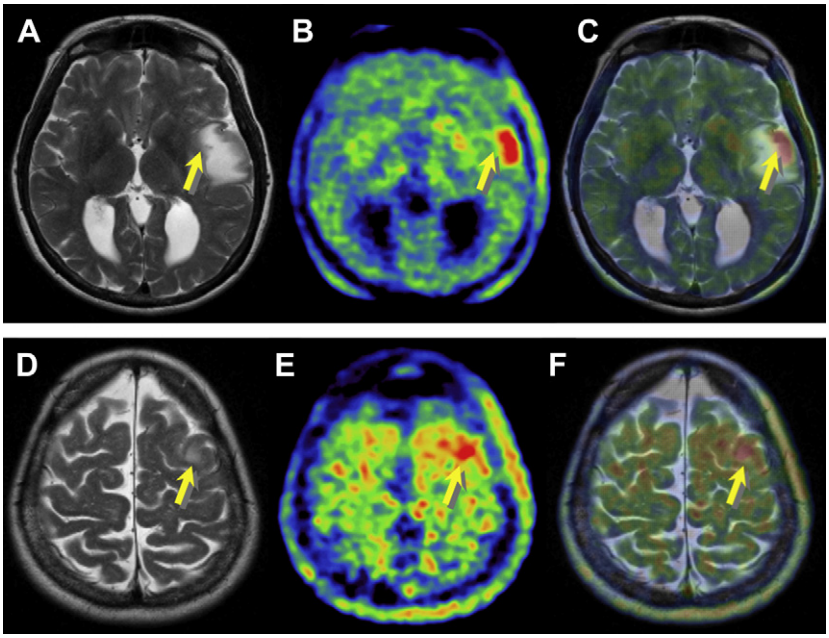

Fig. 7. Example of a patient with a glioblastoma (WHO IV) in the left temporal and frontal areas. The images shown on the *top row* (temporal area) correspond to gadolinium-enhanced T2-weighted MR imaging (*A*), coregistered ^{18}F-FET (*B*), and fused PET-MR (*C*) of the first study. The same is shown in the *bottom row* for the same study in the frontal area (*D–F*). The ^{18}F-FET PET study revealed an additional lesion missed on MR imaging. In addition, the T2-weighted MR imaging and the ^{18}F-FET PET show substantially different gross tumor volume extension for radiation therapy treatment planning. (*Adapted from* Zaidi H, Senthamizhchelvan S. Assessment of biologic target volume using positron emission tomography in high-grade glioma patients. In: Hayat E, editor. Tumors of the central nervous system. vol. 2. New York: Springer; 2011:131–41.)

and intratumoral special distribution of hypoxia are excellent for therapy decision making; however, it is worth mentioning that the tumor-to-blood ratio is generally low in hypoxia imaging, which may translate into statistical uncertainties in measuring intratumoral hypoxic regions.[62] PET imaging of tumor hypoxia has been identified as a prognostic biomarker.[63,64] In addition, the spatial distribution of hypoxic regions within the tumors can guide biologically based radiotherapy treatment planning.[65] In gliomas, there is increasing evidence that tumor hypoxia correlates with radioresistance and the extent of hypoxia in gliomas before radiotherapy is related to decrease in tumor progression time or patient survival time.[66,67] ^{18}F-FMISO imaging of hypoxic glioma cells shows significant promise; however, larger patient population studies are required to ascertain its clinical impact. Identifying the regional distribution of hypoxia may improve planning of resections and allow targeting higher doses of radiotherapy more precisely to the hypoxic areas.

SUMMARY AND FUTURE PERSPECTIVES

Multimodality imaging has become an integral part in the medical management of brain tumors for the past 2 decades. Hybrid PET-MR technology is a major breakthrough and offers many quantitative avenues for brain tumor assessment and quantification. PET imaging provides the opportunity to image noninvasively many biologic processes. Regional biologic information and pathophysiology of brain tumors can be obtained by studying energy metabolism, AA transport, hypoxia, proliferation, and cell death. In radiation oncology, image-guided patient-specific treatment planning has become standard practice, making use of high-precision dose-delivery techniques; however, the success of image-guided radiotherapy is directly related to the accuracy of imaging methods in distinguishing tumors from surrounding normal tissues, which makes PET-MR an essential imaging modality. Studying tumor biology at the molecular level using PET-MR will help in charting personalized treatment plans for patients with brain tumors and also in exploring new therapeutic opportunities in the future.

ACKNOWLEDGMENTS

This work was supported by the Swiss National Science Foundation under grants SNSF

31003A-125246, 33CM30-124114, Geneva Cancer League, and the Indo-Swiss Joint Research Program ISJRP 138866.

REFERENCES

1. DeAngelis LM. Brain tumors. N Engl J Med 2001; 344(2):114–23.
2. Kircher MF, de la Zerda A, Jokerst JV, et al. A brain tumor molecular imaging strategy using a new triple-modality MRI-photoacoustic-raman nanoparticle. Nat Med 2012;18(5):829–U235.
3. Schwenzer NF, Stegger L, Bisdas S, et al. Simultaneous PET/MR imaging in a human brain PET/MR system in 50 patients—current state of image quality. Eur J Radiol 2012;81(11):3472–8.
4. Walter F, Cloughesy T, Walter MA, et al. Impact of 3,4-Dihydroxy-6-18F-Fluoro-L-Phenylalanine PET/CT on managing patients with brain tumors: the referring physician's perspective. J Nucl Med 2012; 53(3):393–8.
5. Dunet V, Rossier C, Buck A, et al. Performance of 18F-fluoro-ethyl-tyrosine (18F-FET) PET for the differential diagnosis of primary brain tumor: a systematic review and metaanalysis. J Nucl Med 2012;53(2): 207–14.
6. Li FM, Nie Q, Wang RM, et al. (11)C-CHO PET in optimization of target volume delineation and treatment regimens in postoperative radiotherapy for brain gliomas. Nucl Med Biol 2012;39(3):437–42.
7. Tan H, Chen L, Guan Y, et al. Comparison of MRI, F-18 FDG, and 11C-choline PET/CT for their potentials in differentiating brain tumor recurrence from brain tumor necrosis following radiotherapy. Clin Nucl Med 2011;36(11):978–81.
8. Slomka P, Baum R. Multimodality image registration with software: state-of-the-art. Eur J Nucl Med Mol Imaging 2009;36(Suppl 1):44–55.
9. Heiss WD, Raab P, Lanfermann H. Multimodality assessment of brain tumors and tumor recurrence. J Nucl Med 2011;52(10):1585–600.
10. Buchbender C, Heusner TA, Lauenstein TC, et al. Oncologic PET/MRI, Part 1: tumors of the brain, head and neck, chest, abdomen, and pelvis. J Nucl Med 2012;53(6):928–38.
11. Shao Y, Cherry SR, Farahani K, et al. Simultaneous PET and MR imaging. Phys Med Biol 1997;42(10):1965–70.
12. Judenhofer MS, Wehrl HF, Newport DF, et al. Simultaneous PET-MRI: a new approach for functional and-morphological imaging. Nat Med 2008;14(4):459–65.
13. Wehrl HF, Sauter AW, Judenhofer MS, et al. Combined PET/MR imaging—technology and applications. Technol Cancer Res Treat 2011;9(1):5–20.
14. Delso G, Furst S, Jakoby B, et al. Performance measurements of the Siemens mMR integrated whole-body PET/MR scanner. J Nucl Med 2011; 52(12):1914–22.
15. Pichler BJ, Kolb A, Nagele T, et al. PET/MRI: paving the way for the next generation of clinical multimodality imaging applications. J Nucl Med 2010; 51(3):333–6.
16. Judenhofer MS, Catana C, Swann BK, et al. PET/MR images acquired with a compact MR-compatible PET detector in a 7-T magnet. Radiology 2007; 244(3):807–14.
17. Schlemmer HP, Pichler BJ, Schmand M, et al. Simultaneous MR/PET imaging of the human brain: feasibility study. Radiology 2008;248(3):1028–35.
18. Herzog H, Pietrzyk U, Shah NJ, et al. The current state, challenges and perspectives of MR-PET. Neuroimage 2010;49(3):2072–82.
19. Zaidi H, Ojha N, Morich M, et al. Design and performance evaluation of a whole-body ingenuity TF PET-MRI system. Phys Med Biol 2011;56(10):3091–106.
20. Holdsworth SJ, Bammer R. Magnetic resonance imaging techniques: fMRI, DWI, and PWI. Semin Neurol 2008;28(4):395–406.
21. Cho ZH, Son YD, Kim HK, et al. A fusion PET-MRI system with a high-resolution research tomograph-PET and ultra-high field 7.0 T-MRI for the molecular-genetic imaging of the brain. Proteomics 2008;8(6): 1302–23.
22. Zaidi H, Schoenahl F, Ratib O. Geneva PET/CT facility: design considerations and performance characteristics of two commercial (Biograph 16/64) scanners. Eur J Nucl Med Mol Imaging 2007; 34(Suppl 2):S166.
23. Zaidi H, Montandon M-L, Assal F. Structure-function based quantitative brain image analysis. PET Clin 2010;5(2):155–68.
24. Zaidi H, Del Guerra A. An outlook on future design of hybrid PET/MRI systems. Med Phys 2011;38(10): 5667–89.
25. Mollet P, Keereman V, Clementel E, et al. Simultaneous MR-compatible emission and transmission imaging for PET using time-of-flight information. IEEE Trans Med Imaging 2012;31(9):1734–42.
26. Zaidi H. Is MR-guided attenuation correction a viable option for dual-modality PET/MR imaging? Radiology 2007;244(3):639–42.
27. Hofmann M, Pichler B, Schölkopf B, et al. Towards quantitative PET/MRI: a review of MR-based attenuation correction techniques. Eur J Nucl Med Mol Imaging 2009;36(Suppl 1):93–104.
28. Zaidi H, Montandon ML, Slosman DO. Magnetic resonance imaging-guided attenuation and scatter corrections in three-dimensional brain positron emission tomography. Med Phys 2003;30(5):937–48.
29. Zaidi H, Montandon ML, Meikle S. Strategies for attenuation compensation in neurological PET studies. Neuroimage 2007;34(2):518–41.
30. Catana C, van der Kouwe A, Benner T, et al. Toward implementing an MRI-based PET attenuation-correction method for neurologic studies on the

MR-PET brain prototype. J Nucl Med 2010;51(9): 1431–8.
31. Keereman V, Fierens Y, Broux T, et al. MRI-based attenuation correction for PET/MRI using ultrashort echo time sequences. J Nucl Med 2010;51(5):812–8.
32. Montandon ML, Zaidi H. Atlas-guided non-uniform attenuation correction in cerebral 3D PET imaging. Neuroimage 2005;25(1):278–86.
33. Hofmann M, Bezrukov I, Mantlik F, et al. MRI-based attenuation correction for whole-body PET/MRI: quantitative evaluation of segmentation- and atlas-based methods. J Nucl Med 2011;52(9):1392–9.
34. Marshall HR, Prato FS, Deans L, et al. Variable lung density consideration in attenuation correction of whole-body PET/MRI. J Nucl Med 2012;53(6): 977–84.
35. Chang T, Clark J, Mawlawi O. A novel approach for the attenuation correction of PET data in PET/MR systems. Med Phys 2012;39(6):3644.
36. Dogdas B, Shattuck DW, Leahy RM. Segmentation of skull and scalp in 3-D human MRI using mathematical morphology. Hum Brain Mapp 2005;26(4): 273–85.
37. Qi J, Leahy RM. Iterative reconstruction techniques in emission computed tomography. Phys Med Biol 2006;51(15):R541–78.
38. Reader AJ, Zaidi H. Advances in PET image reconstruction. PET Clin 2007;2(2):173–90.
39. Tang J, Rahmim A. Bayesian PET image reconstruction incorporating anato-functional joint entropy. Phys Med Biol 2009;54(23):7063–75.
40. Zaidi H, Ruest T, Schoenahl F, et al. Comparative assessment of statistical brain MR image segmentation algorithms and their impact on partial volume correction in PET. Neuroimage 2006;32(4): 1591–607.
41. Matsuda H, Ohnishi T, Asada T, et al. Correction for partial-volume effects on brain perfusion SPECT in healthy men. J Nucl Med 2003;44(8):1243–52.
42. Wang H, Fei B. An MR image-guided, voxel-based partial volume correction method for PET images. Med Phys 2012;39(1):179–95.
43. Shidahara M, Tsoumpas C, Hammers A, et al. Functional and structural synergy for resolution recovery and partial volume correction in brain PET. Neuroimage 2009;44(2):340–8.
44. Le Pogam A, Hatt M, Descourt P, et al. Evaluation of a 3D local multiresolution algorithm for the correction of partial volume effects in positron emission tomography. Med Phys 2011;38(9):4920–3.
45. Daou D. Respiratory motion handling is mandatory to accomplish the high-resolution PET destiny. Eur J Nucl Med Mol Imaging 2008;35(11):1961–70.
46. van der Kouwe AJ, Benner T, Dale AM. Real-time rigid body motion correction and shimming using cloverleaf navigators. Magn Reson Med 2006; 56(5):1019–32.
47. Chun SY, Reese TG, Ouyang J, et al. MRI-based nonrigid motion correction in simultaneous PET/MRI. J Nucl Med 2012;53(8):1284–91.
48. Tsoumpas C, Mackewn JE, Halsted P, et al. Simultaneous PET-MR acquisition and MR-derived motion fields for correction of non-rigid motion in PET. Ann Nucl Med 2010;24(10):745–50.
49. Catana C, Benner T, van der Kouwe A, et al. MRI-assisted PET motion correction for neurologic studies in an integrated MR-PET scanner. J Nucl Med 2011;52(1):154–61.
50. Waldman AD, Jackson A, Price SJ, et al. Quantitative imaging biomarkers in neuro-oncology. Nat Rev Clin Oncol 2009;6(8):445–54.
51. Garibotto V, Heinzer S, Vulliemoz S, et al. Clinical applications of hybrid PET/MR in neuroimaging. Clin Nucl Med 2012 in press.
52. Heinzel A, Stock S, Langen KJ, et al. Cost-effectiveness analysis of amino acid PET-guided surgery for supratentorial high-grade gliomas. J Nucl Med 2012;53(4):552–8.
53. Zaidi H, El Naqa I. PET-guided delineation of radiation therapy treatment volumes: a survey of image segmentation techniques. Eur J Nucl Med Mol Imaging 2010;37(11):2165–87.
54. Weber DC, Zilli T, Buchegger F, et al. [(18)F]Fluoroethyltyrosine- positron emission tomography-guided radiotherapy for high-grade glioma. Radiat Oncol 2008;3(1):44.
55. Vees H, Senthamizhchelvan S, Miralbell R, et al. Assessment of various strategies for 18F-FET PET-guided delineation of target volumes in high-grade glioma patients. Eur J Nucl Med Mol Imaging 2009;36(2):182–93.
56. Weber WA, Wester HJ, Grosu AL, et al. O-(2-[F-18] fluoroethyl)-L-tyrosine and L-[methyl-C-11]methionine uptake in brain tumours: initial results of a comparative study. Eur J Nucl Med 2000;27(5): 542–9.
57. Grosu AL, Weber WA, Riedel E, et al. L-(methyl-11C) methionine positron emission tomography for target delineation in resected high-grade gliomas before radiotherapy. Int J Radiat Oncol Biol Phys 2005; 63(1):64–74.
58. Grosu AL, Weber WA, Franz M, et al. Reirradiation of recurrent high-grade gliomas using amino acid PET (SPECT)/CT/MRI image fusion to determine gross tumor volume for stereotactic fractionated radiotherapy. Int J Radiat Oncol Biol Phys 2005;63(2): 511–9.
59. Galldiks N, Langen KJ, Holy R, et al. Assessment of treatment response in patients with glioblastoma using O-(2-18F-Fluoroethyl)-L-Tyrosine PET in comparison to MRI. J Nucl Med 2012;53(7):1048–57.
60. Piroth MD, Holy R, Pinkawa M, et al. Prognostic impact of postoperative, pre-irradiation F-18-fluoroethyl-L-tyrosine uptake in glioblastoma patients

treated with radiochemotherapy. Radiother Oncol 2011;99(2):218–24.
61. Krohn KA, Link JM, Mason RP. Molecular imaging of hypoxia. J Nucl Med 2008;49(Suppl 2):129S–48S.
62. Carlin S, Humm JL. PET of hypoxia: current and future perspectives. J Nucl Med 2012;53(8):1171–4.
63. Vaupel P, Hockel M, Mayer A. Detection and characterization of tumor hypoxia using pO2 histography. Antioxid Redox Signal 2007;9(8):1221–35.
64. Chitneni SK, Palmer GM, Zalutsky MR, et al. Molecular imaging of hypoxia. J Nucl Med 2011;52(2): 165–8.
65. Ling CC, Humm J, Larson S, et al. Towards multidimensional radiotherapy (MD-CRT): biological imaging and biological conformality. Int J Radiat Oncol Biol Phys 2000;47(3):551–60.
66. Spence AM, Muzi M, Swanson KR, et al. Regional hypoxia in glioblastoma multiforme quantified with [18F]fluoromisonidazole positron emission tomography before radiotherapy: correlation with time to progression and survival. Clin Cancer Res 2008;14(9):2623–30.
67. Bloom HJ. Intracranial tumors: response and resistance to therapeutic endeavors, 1970–1980. Int J Radiat Oncol Biol Phys 1982;8(7):1083–113.